chrna3 modulates biphasic response to alcohol

Authors

Joshua Raine[1], Caroline Kibat [1, 2, #], Tirtha Das Banerjee [3], Antónia Monteiro[3], Ajay S. Mathuru [1, 2, 4, 5, 6 *]

Affiliations

1. Department of Physiology, Yong Loo Lin School of Medicine, National University of Singapore, Singapore, Singapore
2. Yale-NUS College, National University of Singapore, Singapore, Singapore
3. Department of Biological Sciences, National University of Singapore, Singapore, Singapore
4. Institute for Digital Medicine (WisDM), Yong Loo Lin School of Medicine, National University of Singapore, Singapore
5. Institute of Molecular and Cell Biology, A*STAR, Singapore, Singapore
6. Healthy Longevity Translational Research Programme, Yong Loo Lin School of Medicine, National University of Singapore, Singapore, Singapore

*****Correspondence: ajay.mathuru@nus.edu.sg # At the time the work was performed

Abstract

Alcohol use disorders (AUDs) are complex phenomena governed by genetics, neurophysiology, environment, and societal structures. New methods to understand the underlying neurogenetics are valuable for designing better prevention and interventional strategies. Here, we used a novel, two-choice self-administration zebrafish assay (SAZA) to isolate the function of nicotinic acetylcholine receptor (nAChR) subunit alpha3 (*chrna3*) in alcohol response. Juvenile zebrafish exhibited a biphasic response when self-administering alcohol that transitioned from attraction to aversion within minutes, suggesting they can regulate exposure to alcohol. This inverted U-shaped self-administration mirrored the effect alcohol has on shoaling behaviour. Exposure to low concentration of alcohol reduced anxiety-like behaviours characterised by decrease in shoal cohesion, while sedative effects became prominent at higher concentrations resulting in reduced locomotion and uncoordinated swimming. In contrast, *chrna3* mutants displayed blunted responses, exhibiting prolonged alcohol self-administration, and increased gregariousness when compared to wild-type fish. These findings suggest that *chrna3* dysfunction increased tolerance to alcohol. In humans, genetic variants that decrease *CHRNA3* function may increase the likelihood of developing alcohol dependence. Thus, our results provide new insights into *chrna3* function, as a potential target for pharmacological manipulation, and highlight the use of non-rodent alternatives to study neurogenetics of development of AUD.

Keywords:

Zebrafish, Preclinical model, Alcohol Use Disorders, SUD, Hormesis, *CHRNA3*

Introduction

Substance Use Disorders (SUDs) due to the abuse of nicotine, alcohol, and opioids are a major global health burden today, with an estimated 162.5 million disability-adjusted life years lost to them globally in 2016 [1–3]. Among SUDs, harmful alcohol use alone contributes to an astonishing estimate of 5.3% of deaths worldwide, that is, over 3 million individuals annually. This is in addition to the 5.1% of global injury and disease burden attributed to alcohol misuse estimated by the WHO in 2022 [1,4–6]. As this appears to be a preventable phenomenon, great efforts continue to be directed to understand the complex web of biological, environmental, and cultural pressures that can lead to unhealthy use of alcohol and alcohol use disorders (AUDs; [1,4,7,8]).

Apart from the measures to counter AUD at a societal level, research to address the gaps in our understanding of the phenomenon at a biological level is still ongoing. Alcohol response in vertebrates is complex, as it engages a diverse range of neuromodulatory systems in the reward processing circuits. It also directly modulates both glutamate and GABA neurotransmission. Several genetic and neurobiological factors have also been identified that contribute to alcohol abuse resulting in AUD [9–11]. A comprehensive understanding of neurobiology and genetics is therefore crucial for developing effective interventions to prevent and treat AUD taking into account individual variation.

Non-human animal models are fundamental for discovering the genetic factors that contribute to development of substance dependence and addiction in humans [12]. Usually, such studies are conducted in mammals, in primates or rodents. They, however, become prohibitive with high operating costs when modelling genetic variability and the small effects of single genes [13,14]. Zebrafish have emerged as a viable alternative in the past decade that overcome some of these limitations as whole-brain neural activity in intact animals can be combined with genetic manipulation for higher throughput [15–18]. Anatomical and functional conservation with the mammalian sub-cortical circuitry associated is also now well established [19–21].

Recent studies showed that behavioural and physiological responses of zebrafish to a range of substances are also consistent with those exhibited by mammals, both on the acute and chronic scale, thus providing grounds for construct validity [22,23]. However, behavioural studies using zebrafish have primarily used indirect measures such as place preference and avoidance assays [24–27]. These are useful but are inadequate to model addiction[12]. Although difficult to design for aquatic animals, contingent assays of self-administration are essential to gain construct and predictive validity for the human condition [12]. Only a few studies other than ours have explored alternatives such as active choice [28], or self-administration [29–31], with ours being suitable for self-administration in younger fish. Performing experiments in younger fish is a specific advantage for throughput when the expected effect size of manipulation is small. These studies collectively demonstrate the potential of zebrafish models for identifying genetic factors underlying substance addiction [29–31] .

Here, we expanded on the use of SAZA - Self-Administration Zebrafish Assay [30] to study the role of *chrna3* in acute response to alcohol. In human genetic studies, single nucleotide polymorphisms (SNPs) at the 15q25 locus containing the gene cluster *CHRNA5-A3-B4* encoding the α5, α3, and β4 nicotinic acetylcholine receptor (nAChR) subunits are consistently associated with nicotine addiction [32–34]. Apart

from the common variants identified in GWAS, rare variants in *CHRNA3* have also been significantly associated with alcohol dependence in humans [35,36]. Investigations into the molecular mechanism connecting *CHRNA5* and *CHRNB4* to SUD have progressed rapidly since initial genetic association studies relying on mutant or knock-out rodent models [37,38]. However, similar models for the third gene in this cluster, *CHRNA3*, are lacking [39,40]. The exact role *CHRNA3* plays in substance dependence is therefore incomplete at present. Our study fills this gap and provides validation that *chrna3* impacts the acute response to alcohol.

Using SAZA for 3-4 week old juvenile zebrafish we first report that the acute response to alcohol is biphasic, transitioning rapidly from attraction to avoidance within minutes. We found that this biphasic response matches the proposed roles of alcohol, operating both as an anxiety reducing agent, or an anxiolytic, as well as a sedative. *chrna3* mutants, however, showed tolerance to alcohol, delaying the transition to alcohol avoidance during self-administration, and resisting changes to their shoaling behaviour during alcohol exposure. In the context of the Genetically Informed Neurobiology of Addiction (GINA), our study provides new evidence that rare missense variations in *CHRNA3* may be directly responsible for a predisposition to alcohol addiction in humans [35,41].

Results

We refined the Self-Administration Zebrafish Assay (SAZA) first reported by Nathan *et al.* (2022) [30] to improve the temporal resolution of behavioural studies. SAZA apparatus created three chemically distinct, but physically continuous zones, or regions within the assay chamber. The inflow and outflow were adjusted by gravity feed to maintain the integrity of the two delivery zones throughout the assay period (Figure S1). Subject fish behaviour was monitored by a closed-loop, video acquisition program developed in-house that allowed for self-administration of a stimulus or a control when subject fish entered a delivery zone via a neutral zone (Figure 1A). To avoid intrinsically preferred swimming direction bias, the stimulus and control delivery zones were pseudo-randomly assigned in each trial such that half of the fish in each group received the stimulus (alcohol) in the left and the other half in the right delivery zone (Figure 1A). Sparkline plots in pilot experiments showed that fish administered 20%, or 70% alcohol (at source) differentially, by changing the frequency of entry, and duration of time spent in the stimulus area (Figure 1B; Video S1). This suggested that fish can self-regulate alcohol administration which can be quantified and their behaviour in the closed-loop setup was dependent on stimulus concentration .

Next, we estimated the stimulus concentration that fish experienced during the assay. To do so, we used a densitometer to measure the change in water density caused by the alcohol-water mixture. Alcohol was dispensed mimicking the behaviour of fish in the pilot experiment (Figure 1B, ~10 seconds/min discontinuously, table S1). This revealed that due an improved outflow and the lower density of the alcohol-water mixture, the concentration of alcohol in the chamber was a fraction of the concentration at the source. It was lower than the estimates provided by colorimetric analysis of food dye-containing solution (Figure 1C). The maximum concentration plateaued at ~40-fold lower than the source alcohol concentration, which is at least four-fold lower than previous studies [30]. Therefore, on an average, self-administering source alcohol at 20% and 70% resulted in the fish experiencing alcohol at ~0.5% and ~1.5% respectively in the assay (Figure 1C; for 20%, $\bar{x}$ = 0.52 %, SD = 0.13%; 70%, $\bar{x}$ = 1.52%, SD = 0.44%). We refer to these two conditions as $\bar{x}$0.5% condition and $\bar{x}$1.5% respectively in the rest of this study.

These range of alcohol exposure is comparable to the concentration of alcohol used in previous zebrafish studies [24,26,27,42]. The effective concentration reduced by half within a minute of stopping self-administration (Figure 1C). Thus, both the pre, and post-administration periods served as controls to compare the behaviour of animals in the naïve, and post exposure periods.

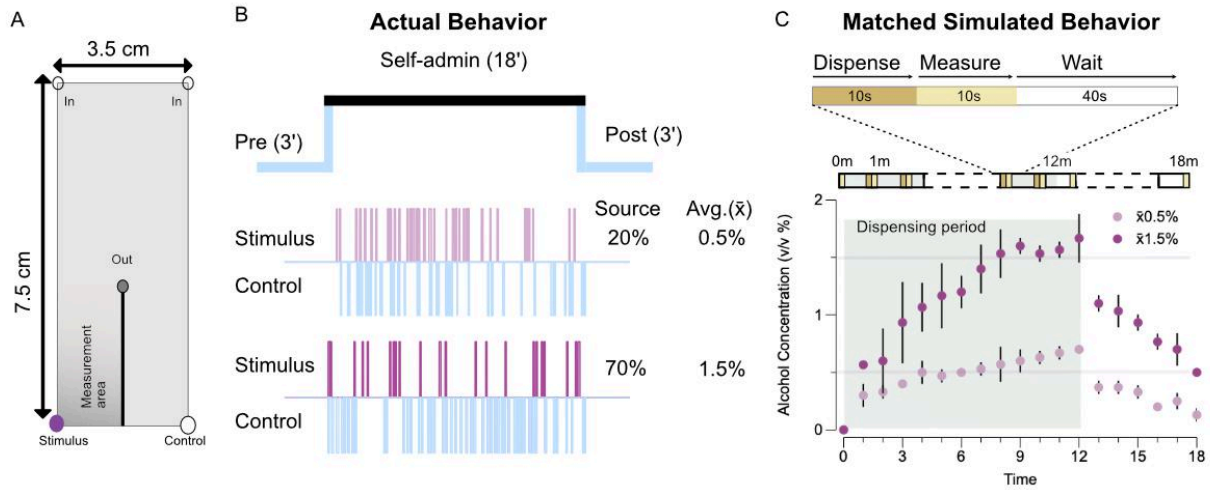

Figure 1. **Self-Administration Zebrafish Assay (SAZA) chamber and functionality**

A. Schematic indicating locations of inflow of system water (In, top) and outflow (Out, centre). Control and stimulus delivery inlets (stimulus shown in purple) are activated when a fish enters the corresponding zone. Continuous inflow and outflow constrain the stimulus/control delivered to their respective zones (Figure S1). 'Measurement area' denotes where alcohol concentration was measured in panel C. **B.** Schematic shows the experimental design with 3m pre- and post-exposure periods before and after an 18m self-administration period. Representative sparklines plots show the entries and duration (thickness) of entry of the subject fish either into the stimulus or the control zones when 20% or 70% alcohol is used as stimuli. **C.** Alcohol concentrations measured when 20% or 70% alcohol were dispensed for the duration mimicking subject fish behaviour (± standard error). The average concentration (solid line) fish experience is 0.5% and 1.5% alcohol respectively. See Table S1 for additional details.

Having established a robust scheme of self-administration we first examined the behaviour of juvenile wild-type fish (WT; 3-4 weeks old) in the SAZA. The pilot (Figure 1B) suggested the preference was dynamic. To capture this dynamism, we collapsed the behaviour of animals over 3-minute intervals. This analysis for the x̄0.5% alcohol condition revealed that fish initially spent significantly more time in the stimulus zone compared to the pre-exposure period (Figure 2A, 3-6m, Cliff's delta = 0.402, 95CI [0.636, 0.093], p = 0.007). However, after about 12 minutes, fish reversed their preference and spent significantly less time in the stimulus zone (Figure 2A, 12-15m, Cliff's delta = 0.43, 95CI [-0.147, -0.673], p = 0.002). This avoidance continued for the remainder of the assay, even after the self-administration period ended. The early attractive portion of this biphasic response was stunted in the x̄1.5% condition, however (Figure 2B, 0-6m, Cliff's delta = 0.0511, 95CI [0.349,-0.24], p = 0.724). Fish spent less time in the stimulus zone from 6 minutes onwards (Figure 2B, 6-9m, Cliff's delta = -0.424, 95CI [-0.12, -0.651], p = 0.005). Comparing the behavioural changes with the alcohol concentration expected in the stimulus zone

revealed that juvenile zebrafish preferred alcohol at ~0.5% or less, but avoided ~0.7% or higher (Figure 2C), Thusm WT zebrafish self-regulated alcohol exposure to a narrow range.

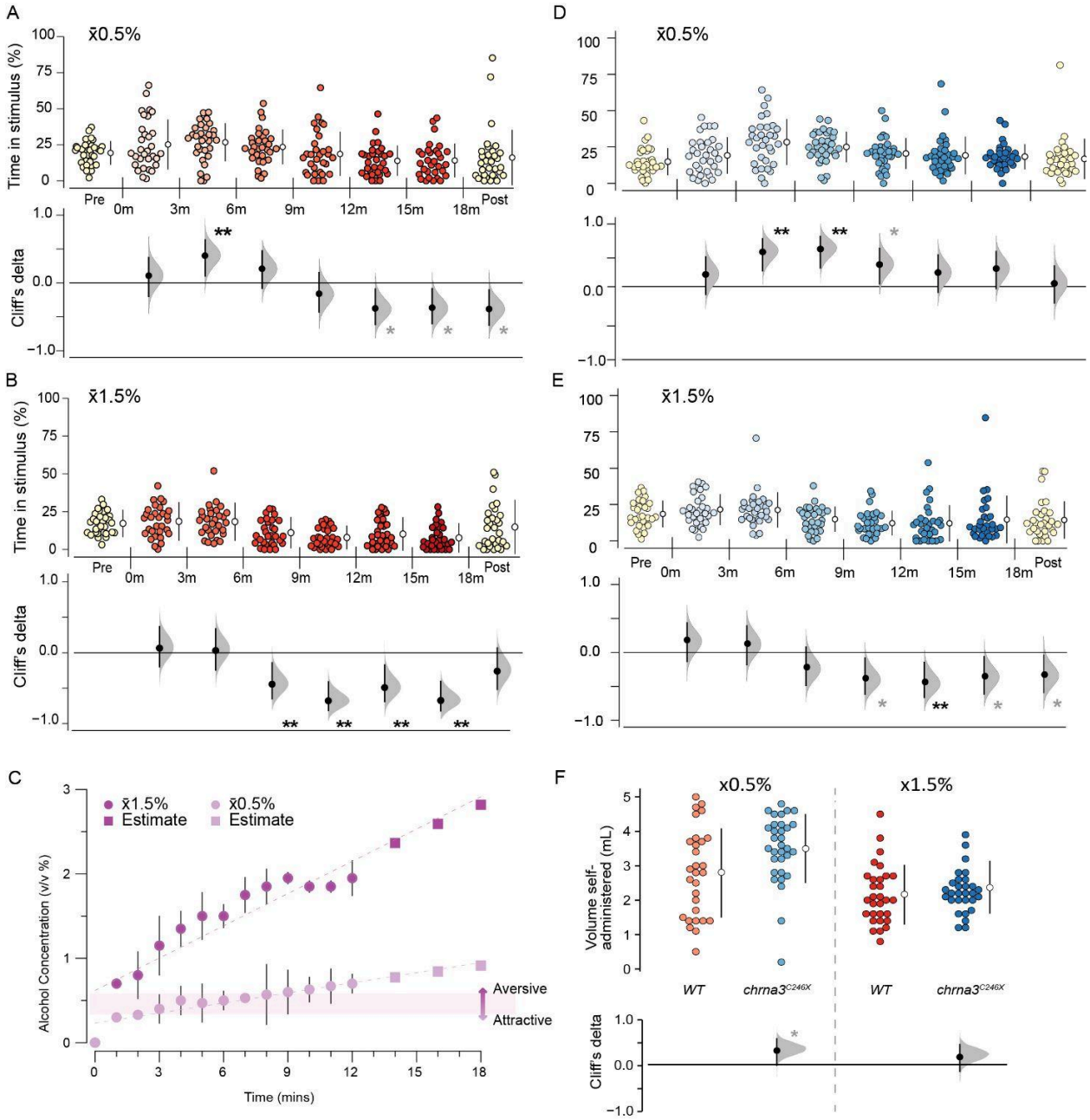

Figure 2. The preference for alcohol is biphasic.

Gardener-Altman and Cumming estimation plots show alcohol response in three-minute intervals. No stimulus was dispensed in the 'Pre' and 'Post' periods. Time spent in the stimulus zone during x̄0.5% SAZA condition for **A.** WT (n = 31) and **D.** *chrna3*^{C246X} mutants (n = 32). Time spent in the stimulus zone in the x̄1.5% SAZA condition **B.** for WT (n = 30). and **E.** for *chrna3*^{C246X} mutants (n = 30). **C.** Ethanol concentrations in the stimulus zone in the x̄0.5% and x̄1.5% alcohol conditions and estimated for

extended periods. The concentration at which attraction switches to aversion is highlighted. **F.** Gardener-Altman and Cumming estimation plot for volume of stimulus self-administered during x̄0.5% or x̄1.5% SAZA conditions comparing WT and *chrna3*^{C246X}. Asterisks indicate a significant difference between that time portion and the pre-stimulus period: * = p < 0.05 and Cliff's delta > ± 0.2 & < ± 0.4 (provisional difference), ** = p < 0.01 and Cliff's delta > ± 0.4 (meaningful difference). See tables S2 and S3 for the precise effect sizes and p-values, corrected for multiple comparisons.

These observations suggest that the SAZA can detect alcohol preference changes in the subject fish at a high temporal resolution. This is a key advantage for untangling the small effects single genes may have on complex behaviours like alcohol preference. Common variants in *CHRNA3*, for example, are a genetic risk for developing nicotine dependence, while several rare variants are proposed to influence cocaine and alcohol dependence [35,43]. *Chrna3* is also proposed as a candidate gene in mediating alcohol stimulant effects in rodents [44]. However, its role in development of alcohol dependence hasn't been tested directly. We hypothesised that the SAZA can be used to detect even subtle effects, if present, in a CRISPR mutant fish line for the nicotinic acetylcholine receptor alpha3 subunit generated recently (Kibat, C. Ph.D. thesis 2021). The *chrna3* mutant had an insertion, a frameshift, and a stop codon in transmembrane region 1 at the amino acid position 246 (*chrna3*^{C246X}; Figure 3A).

The mutant protein is predicted to have a large truncation of the transmembrane and the intracellular domains (Figure 3B) and is thus expected to be damaging to protein function. Quantitative RT-PCR of adult whole brains showed that the mutation resulted in a significant reduction in the expression of *chrna3* transcripts in the mutants (Figure 3C, *WT* vs. *chrna3*^{C246X}, Cliff's delta = -0.848, 95CI [-0.567, -0.962], *p* = < 0.001). In rodents, *Chrna3* expression is restricted. It is expressed in a few neurons in the hippocampus, medial habenula, Interpeduncular Nucleus (IPN), the VTA, cerebellum, locus coeruleus, and spinal cord [45,46]. We examined the expression of zebrafish *chrna3* in the 14 dpf zebrafish larvae using an HCR™ RNA-FISH (HCR) method modified in-house (Figure 3D-F). Only a few cells in the left dorsal habenula expressed *chrna3* at a low level at this age. The expression levels in the mutant and WT were similarly low (Figure 3E, S2). However, the expression of *chrna3* was starkly reduced in the hindbrain and a few midbrain regions (Figure 3F, S3).

We next examined the behaviour of *chrna3*^{C246X} mutants in the SAZA. In the x̄0.5% condition, *chrna3*^{C246X} fish initially behaved like their WT counterparts, spending significantly more time in the stimulus zone in the first half of the self-administration period (Figure 2D, pre vs. 6-9m, Cliff's delta = 0.568, 95CI [0.761, 0.281], *p* = < 0.001). However, unlike the WT fish, the attraction persisted for longer (Figure 2D, 9-12m, Cliff's delta = 0.334, 95CI [0.588, 0.039], *p* = 0.018, S4A). In addition, the response did not switch to avoidance. This increase in alcohol tolerance was paralleled by an increase in the volume of the alcohol self-administered (Figure 2F, x̄0.5%, Cliff's delta = 0.328, 95CI [0.584, 0.009], *p* = 0.027). In the x̄1.5% condition, mutants unlike WT displayed a notable avoidance only from 9-12m (Figure 2E, 3-6m, Cliff's delta = 0.118, 95CI [0.411, -0.187], *p* = 0.428, 12-15m, Cliff's delta = -0.447, 95CI [-0.156, -0.68], *p* = 0.003). Therefore, although the shape of the dose-response curve was similar to WT (Figure 2E), it was shifted rightwards with the onset of aversion delayed (Figure 2E, 6-9m, Cliff's delta = -0.229, 95CI [0.082, -0.493], *p* = 0.128, S4B).

Despite the early attraction (Figure 2A, 2D), alcohol appeared to be aversive to zebrafish in general, albeit less so for the mutants. This could also be inferred from the volumes of alcohol delivered relative to the volume of control (0% alcohol). WT fish self-administered significantly smaller volumes alcohol in the x̄0.5% condition (Figure 4A, Cliff's delta = -0.554, 95CI [-0.266, -0.759], p = <0.001), and in the x̄1.5% condition (Figure 4A, Cliff's delta = -0.728, 95CI [-0.441, -0.895] p = <0.001). This supports previous observations that alcohol can be aversive to zebrafish at certain concentrations [30]. The *chrna3*^{C246X} mutant fish however, reduced volume of administration only in the x̄1.5% condition (Figure 4B, 0% vs x̄1.5%, Cliff's delta = -0.583, 95CI [-0.304, -0.791], p = <0.001), corroborating the increased time seen in the stimulus zone in the x̄0.5% condition (Figure 2D).

To quantify the magnitude of preference, previous studies used a Preference Index (or PI [30]). PI was defined as the ratio of the difference between the time spent in the stimulus and control zones relative to the total time spent in the two zones. Positive PI values (0 to +1) thus indicated a preference for stimuli, while negative values (0 to -1) indicated an aversion. To quantify the magnitude of change in preference over time, here we quantified the change in PI, or a delta PI (ΔPI) between different phases of the experiment. We compared the pre-exposure phase, the early phase (0-9 minutes), and the late phase (9-18 minutes) of self-administration. In WT fish, the ΔPI between the pre-exposure and the early phase showed a significant increase only for x̄0.5% condition (Figure 4C, Cliff's delta = 0.317, 95CI [0.577, 0.014], p = 0.038). On the other hand, the ΔPI decreased significantly only for x̄1.5% condition between early and late phases (Figure 4E, Cliff's delta = -0.504, 95CI [-0.227, -0.724], p = < 0.001). In contrast, the mutants exhibited a positive ΔPI from pre-exposure to the early phase under both conditions (Figure 4D, 0 vs x̄0.5%, Cliff's delta = 0.449, 95CI [0.127, 0.682], p = 0.002; 0 vs x̄1.5%, Cliff's delta = 0.412, 95CI [0.108, 0.647], p = 0.007), while the ΔPI indicating aversion was marginal (Figure 4F, 0 vs x̄1.5%, Cliff's delta = -0.201, 95CI [-0.095, -0.493], p = 0.192). In addition to the increased alcohol tolerance, the mutants also exhibited heightened alcohol-induced locomotor stimulation, especially under x̄0.5% conditions, over the full stimulus-dispensing period (Figure S5) that impacted other behavioural characteristics of the mutants (Figure S6). Taken together, these results suggest that *chrna3*^{C246X} mutants primarily differed from the WT fish in their tolerance to concentrations of alcohol that are aversive.

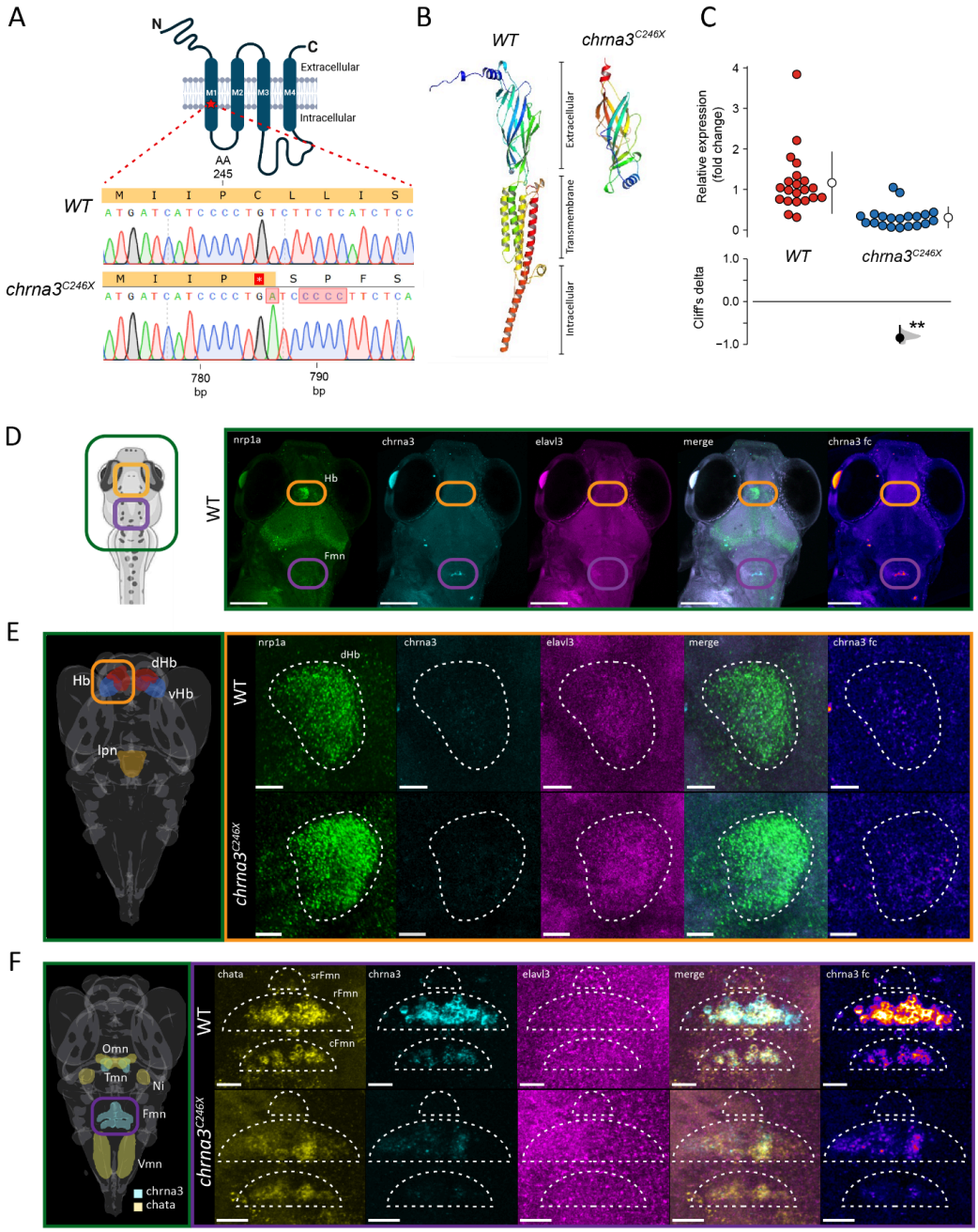

Figure 3. **Characterisation of the *chrna3*^{C246X} mutant zebrafish.**

A. *chrna3*^{C246X} mutant fish have a premature stop codon in the transmembrane region 1, amino acid 246 (M1 - red star), due to the indel of 5bp at position 786bp. **B.** Predicted protein structure of Chrna3 in WT and *chrna3*^{C246X} mutants, generated by iTasser [47], colour coded by domain. **C.** Fold change of *chrna3* in WT (n = 21) vs. *chrna3*^{C246X} (n = 20) by qRT-PCR. **D-F.** *chrna3* expression in 14dpf zebrafish larvae

visualised by HCR™ RNA-FISH (HCR). **D.** Overview of the zebrafish whole brain. **E.** Higher resolution images of the dorsal habenula (dHb) marked by *nrp1a* expression and **F.** Predicted facial motor nucleus (Fmn) marked by *chata* expression, in WT and *chrna3*^{C246X} respectively. Schematic images with regional markers (v2.0, MECE, 2024) were generated in mapZeBrain Atlas (mapzebrain.org, July 2024) [48]. Hb = habenula, vHb = ventral habenula, Ipn = interpeduncular nucleus, , Omn = oculomotor nucleus, Trm = trochlear motor nucleus, Ni = nucleus isthmi, Vmn = vagus motor nucleus, srFmn = supra-rostral Fmn, rFmn = rostral Fmn, cFmn = caudal Fmn. Genes presented left to right: *nrp1a* (**E**) or *chata* (**F**), *chrna3*, *elavl3,* these three genes merged, and *chrna3* with false colour post-processing. False colour adjusted (fc) and elavl3 images have been brightened for enhanced visibility. Scale bars: **D** = 200µm, **E** = 20 µm, **F** = 20 µm.

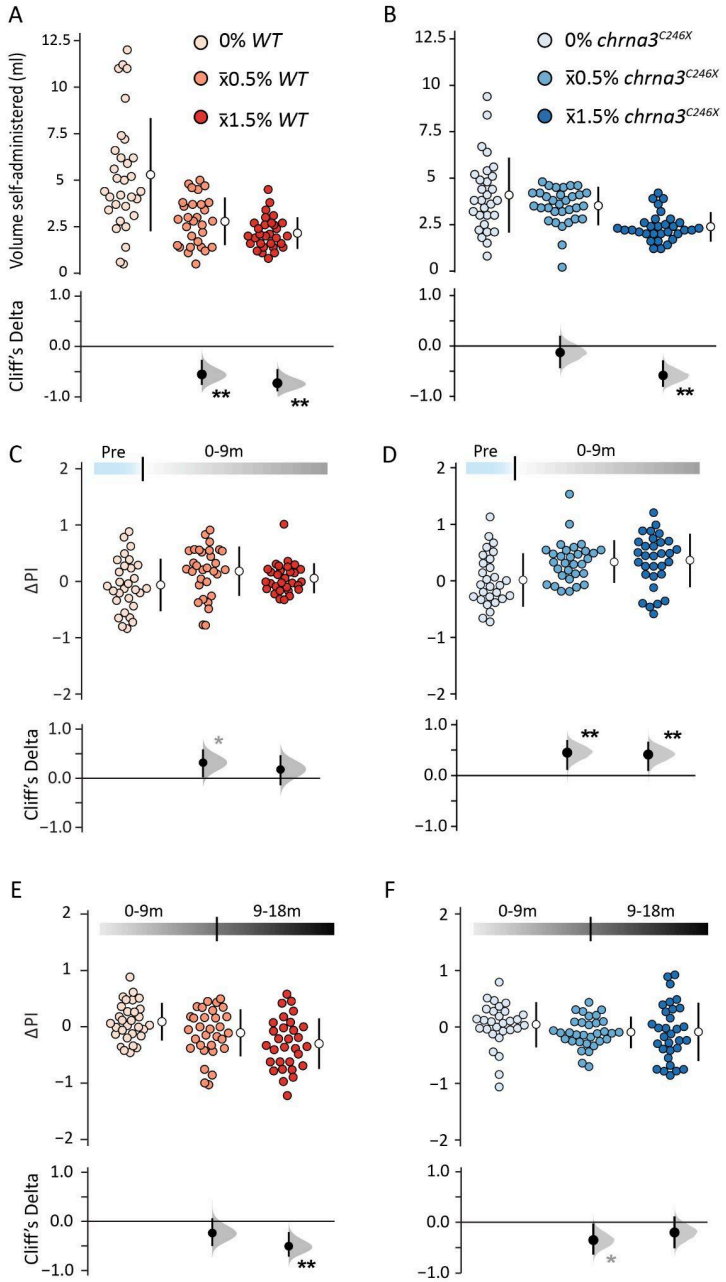

Figure 4. *chrna3* mutation alters relative preference for alcohol.

Gardener-Altman and Cumming estimation plots for SAZA for WT (**A, C, E**) and *chrna3*^{C246X} (**B, D, F**). Plots show comparison of different alcohol concentrations (0%/x̄0.5%/x̄1.5%) for WT (n = 31/31/30), and *chrna3*^{C246X} (n = 29/32/31). Asterisks indicate the following significant differences from 0% alcohol treatments: * = $p < 0.05$, and effect size reported by Cliff's delta between ± 0.2 and ± 0.4 are considered provisional, ** = $p < 0.01$ and effect size bigger than ± 0.4 is considered a meaningful difference. **A, B)** The volume of stimulus self-administered by wild type and *chrna3*^{C246X} mutants respectively. **C, D)** Change in preference index (ΔPI) from the pre-exposure period to 0-9m of the stimulus delivery period by wild type and *chrna3*^{C246X} mutants respectively. **E, F)** Change in preference index (ΔPI) of zebrafish from 0-9m to 9-18m of the stimulus delivery period by wild type and *chrna3*^{C246X} mutants respectively. See Table S5 for the exact effect size and p-values.

We next explored the potential reasons for this rapid and biphasic response to alcohol self-administration. Alcohol is well-documented to act as an anxiolytic, reducing a variety of anxiety-like behaviours in fish [49,50]. However, it is also known to function as a sedative, causing reduced swimming velocity and coordination, and increased immobility [24,26,51]. We hypothesised that the biphasic response in SAZA is correlated to the concentrations at which these two contrasting effects of alcohol come into play. To test this, we examined the shoaling behaviour of juvenile fish. Shoal members are proposed to swim near others when anxious and are expected to be more exploratory when the anxiety-like state is reduced [52]. This will be reflected in the total area occupied by the shoal. On the other hand, shoal members experiencing the sedative effects of alcohol are expected to swim with decreased speed and coordination. This impacts the distance covered by the shoal, or the shoal kinesis, irrespective of the total area occupied by the shoal. Hence, the impact of both the anxiolytic and sedative effects of alcohol can be measured by examining shoaling behaviour.

Taking into account the concentrations associated with attraction and aversion (Figure 2C), we examined the shoaling behaviour of four fish over 30 minutes at two fixed concentrations of 0.5%, or 1% alcohol and compared their behaviour when alcohol was absent (0%; Figure 5A, Video S2). The total area between WT shoal members increased at both concentrations, with the 1% alcohol having a proportionally larger effect on the shoal area (Figure 5B, 0 vs 0.5%, Cliff's delta = 0.379, 95CI [0.423, 0.332], p = <0.001, 0 vs 1%, Cliff's delta = 0.518, 95CI [0.559, 0.475] p = <0.001). The same phenomenon was also observable in the mutants (Figure 5C, 0 vs 0.5%, Cliff's delta = 0.365, 95CI [0.412, 0.320], p = <0.001, 1%, Cliff's delta = 0.611, 95CI [0.649, 0.573] p = <0.001).

Differences between the two genotypes emerged when their behaviours were examined at a higher temporal resolution. Loss of cohesion in WT fish was observable within five minutes of exposure to either concentration (Figure 5D, 0 vs 0.5% 3-6m, Cliff's delta = 0.287, 95CI [0.320, 0.252], p = < 0.001; Figure 5D 0 vs 1% 3-6m, Cliff's delta = 0.338, 95CI [0.370, 0.305], p = < 0.001). The magnitude of the difference increased over time (Figure 5D, 0 vs 0.5% 12-15m, Cliff's delta = 0.552, 95CI [0.579, 0.522], p = < 0.001; 0 vs 1% 12-15m, Cliff's delta = 0.728, 95CI [0.749, 0.707], p = < 0.001). We quantified shoal kinesis as the distance between the shoal centre point at 2 fps (Figure 5F). Shoal kinesis changed negligibly over time with 0.5% alcohol treatment, while it was reduced almost immediately with 1% alcohol treatment. The effect became larger over time (Figure 5F, 0 vs 1%, 6-9m, Cliff's delta = -0.419, 95CI [-0.387, -0.449], p = < 0.001). Thus, immersion in 0.5% alcohol reduced anxiety-like behaviours, while sedative-like effects were more evident when immersed in 1% alcohol (Figure 5D, 5F).

The *chrna3*^{C246} mutants seemed to experience the effects of alcohol exposure differently. Behaviour of unexposed (0% alcohol) was similar between the two genotypes with the *chrna3*^{C246X} exhibiting slight differences in shoal cohesion (Figure S7A), and shoal kinesis (Figure S7B). However, unlike the WT shoals, exposure to 0.5% alcohol reduced shoal cohesion only marginally (Figure 5E) and it did not increase over time as it did in the WTs (Figure 5E). This difference is clearer when genotypes are compared directly. Mutant fish retained significantly tighter shoaling cohesion compared to the wild type (Figure 5H, 12-15m, Cliff's delta = -0.44, 95CI [-0.409, -0.47], p = < 0.001). Meanwhile, shoal kinesis was initially heightened in *chrna3*^{C246X} fish compared to the WTs (Figure 5I, 0-3m, Cliff's delta = 0.253, 95CI [0.288, 0.219], p = < 0.001), which paralleled the *chrna3*^{C246X} alcohol-induced motility stimulation in the SAZA (Figure S5). The alcohol-induced kinesis difference between genotypes gradually declined as the assay

progressed (Figure 5I). This divergence in behaviours between genotypes suggests that the anxiolysis from the alcohol exposure was much lower in *chrna3*^{C246X} than that experienced by their WT counterparts.

The behaviour differences between the mutant and wild-type shoals were minimal in 1% alcohol for the majority of the assay duration (Figure S7C). However, in the latter part of the assay mutants seemed to resist the sedative effects of alcohol, retaining higher shoal kinesis than the wild type (Figure S7D, 15-18m, Cliff's delta = 0.372, 95CI [0.405, 0.34], p = < 0.001). The effects of alcohol on shoal cohesion and kinesis in the first five minutes of exposure were similar between genotypes (Figure S8, S9). Overall, these results from the shoaling assay suggest that *chrna3*^{C246X} had reduced effect of alcohol exposure on anxiolysis as well as sedative effects seen in WT fish.

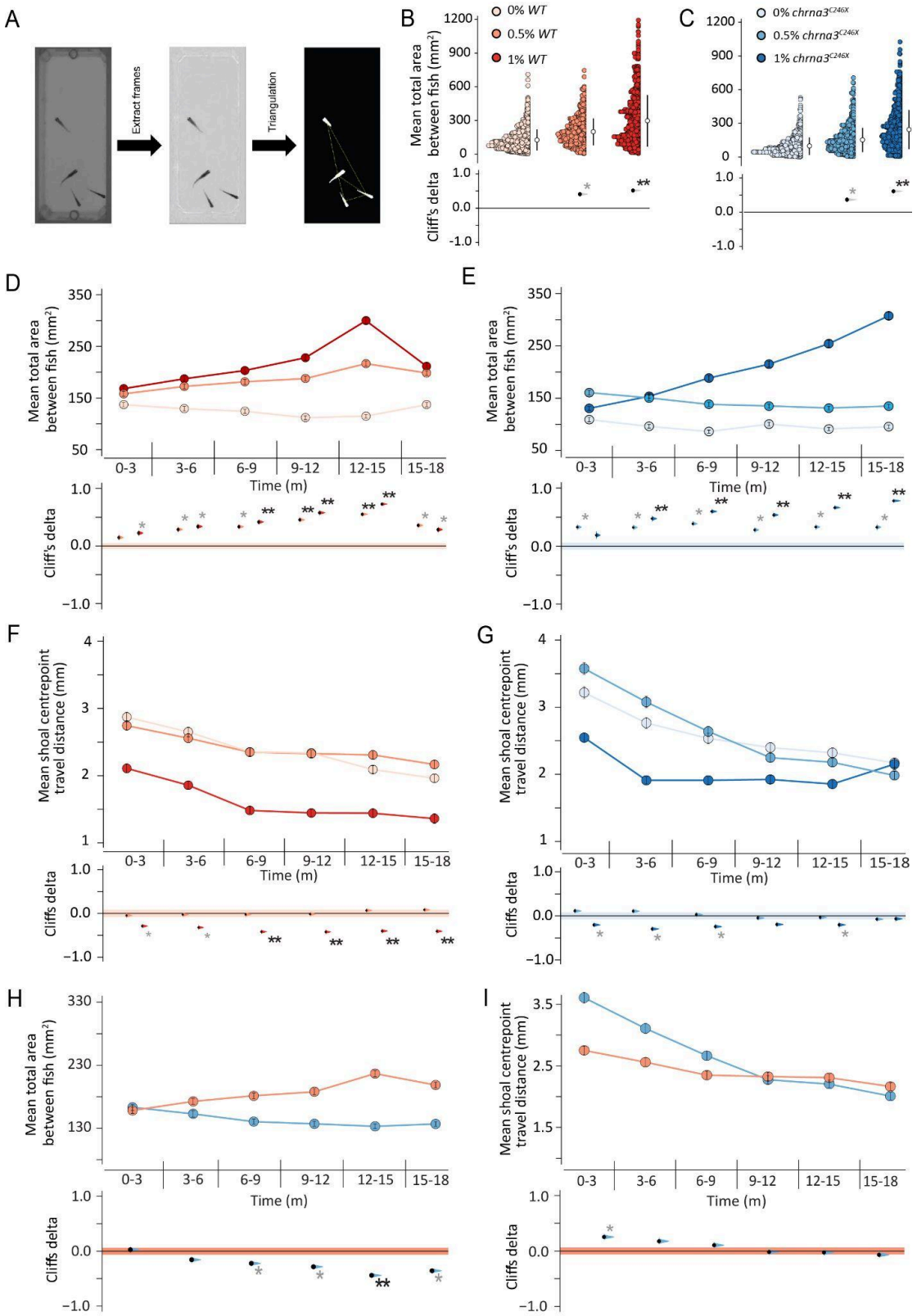

Figure 5. *chrna3* mutants experience reduced anxiolysis from alcohol exposure. Gardener-Altman (**B, C**), or mean (± 95% CI) shoal cohesion (**D, E, H**) and kinesis (**F, G, I**), and Cumming estimation plots for the

shoaling cohesion assay showing WT (**B, F, H**), *chrna3*^{C246X} (**C, E, G**), and comparisons (**H, I**). Metrics compared per frame at 2fps (n = 6 assays per genotype, per treatment). Asterisks indicate the following significant differences from 0% alcohol (**B-G**) or WT (**H, I**) within that time: * = $p < 0.05$, and effect size reported by Cliff's delta between ± 0.2 and ± 0.4 are considered provisional, ** = $p < 0.01$ and effect size bigger than ± 0.4 is considered a meaningful difference. See tables S9 and S10 for exact effect size and p-values. **A)** Schematic outline of the shoaling cohesion assay and processing. **B, C)** The total area between wild type and *chrna3*^{C246X} fish, respectively, over 30 minutes of alcohol immersion. **D, E, H)** The mean total area between wild type and *chrna3*^{C246X} fish, respectively, over 18 minutes of alcohol exposure by three-minute intervals. **F, G, I)** The mean shoal centrepoint travel distance per frame between wild type and *chrna3*^{C246X} fish, respectively, over 18 minutes of alcohol exposure by three-minute intervals.

To gain an understanding of these behavioural differences we performed bulk RNA sequencing of WT and mutant whole brains. Differential gene expression (DEG) analysis suggested that the two genotypes had large differences, with PC1 accounting for ~44% of the variation in a PCA (Figure 6A). In total, the expression of ~1600 genes was significantly changed (2-fold or more), and a further ~4600 genes were identified with provisional alterations (less than 2 fold; Figure 6C). Of these, there was an approximately even split between up- and down-regulated gene numbers (Figure 6C). Gene Set Enrichment Analysis (GSEA) revealed notable enrichment in transcriptional changes in mutants (Figure 6B). The significantly enriched biological functions impacted in the mutant included neuronal development, ion channel function, and secondary messenger-associated processes (Figure 6B). Additionally, genes associated with feeding behaviour were also enriched. This perhaps indicates a wide cascade of compensatory changes induced by the reduced expression and function of *chrna3.*

Major neurotransmitter signalling including glutamate, and GABA receptors in addition to nAChRs, which are activated by exposure to psychoactive substances like alcohol, also showed modest changes in expression patterns (Figure 6D-F). Both glutamate and GABA receptors appeared to show a small but consistent upregulation amongst many receptor subunits (Figure 6D-E). The expression of most nAChR genes however was unchanged, though a few were positively or negatively regulated with no consistent trend (Figure 6F). Closer inspection of the nAChR subunit gene counts revealed that expression was very low for some subunits, as was highlighted for *chrna3* in the HCR (Figure 3, 6G). For genes with low expression counts it is a challenge to determine significant changes through RNA-seq analysis. As *CHRNA3* expression is co-regulated with *CHRNA5* and *CHRNB4* in mammals, both of which have also been associated with substance use disorders, we examined whether the expression of these genes had also been altered in the mutant. Both *chrna5* and *chrnb4* displayed significant downregulation by qPCR, with the effect size being much larger for the latter (Figure 6H).

We also examined gene sets curated from meta-analyses of genes consistently associated with alcohol and nicotine dependence in humans [53], and with mammalian anxiety phenotypes [54,55] to address whether *chrna3* dysfunction also alters expression of these genes (Figure 6I-K). The alcohol dependence-associated genes exhibited few changes (Figure 6I), however, ~50% of the nicotine-dependence genes were provisionally upregulated in the mutant (Figure 6J). Finally, genes associated with anxiety phenotypes also showed a number of expression changes, albeit some in positive and some in negative direction of expression (Figure 6K). In all cases, this analysis revealed that

though the expression of a large number of these genes changed they were modest (Figure S10, Table S15).

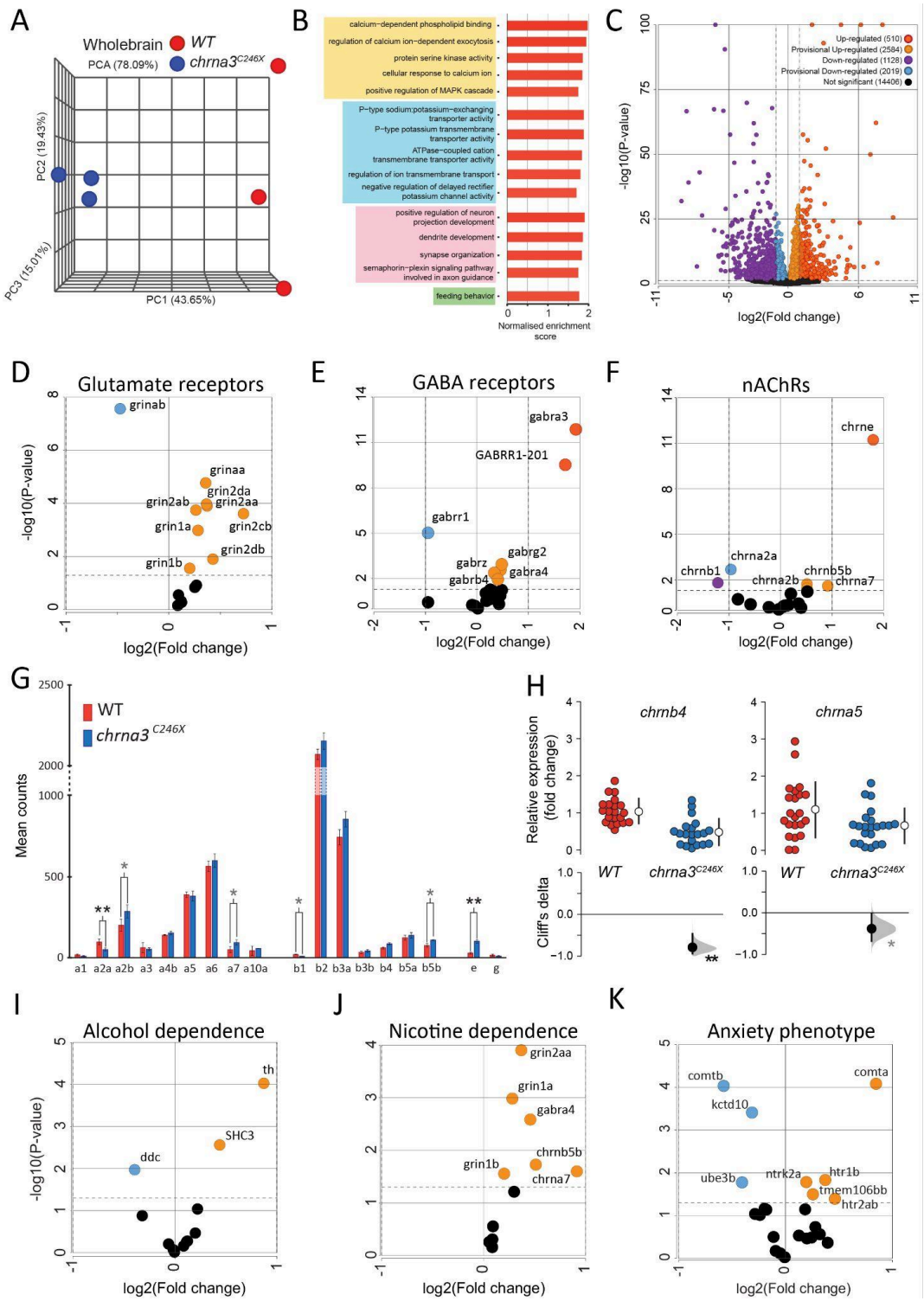

Figure 6. *chrna3^{C246X}* mutants exhibit transcriptional changes in dependence, neuronal development, and ion channel process associated genes. RNAseq comparison of *chrna3^{C246X}* (n = 3) vs *chrna3^{C246X}* (n = 3) zebrafish whole brain tissues. **A.** PCA clustering of samples by genotype. **B.** All significantly enriched

GO terms between genotypes. Positive enrichment values indicate enrichment in the *chrna3*^{C246X} mutant zebrafish. Significance thresholds are defined at $p = < 0.05$ and FDR < 0.2. Yellow = secondary messenger associated, Blue = ion channel associated, pink = neuronal differentiation and development, green = behaviours. **C.** Volcano plot of gene expression changes between genotypes. Up/down-regulated genes = $p < 0.05$ & log2 fold change > ±2. Provisional up/down-regulated genes = $p < 0.05$ & log2 fold change < ±2. Not significant genes = $p > 0.05$. The colour key applies to D-F and I-K. Positive fold change values indicate up-regulation in the *chrna3*^{C246X} mutant zebrafish. **D-F.** Subsets of volcano plot **C**, highlighting glutamate **(D)**, GABA **(E)** and nicotinic acetylcholine (nAChR) **(F)** receptor gene families. **(G)** Mean counts (± standard deviation) of nAChRs (gene prefix 'chrn'). Stars indicate significant difference between genotypes, ** = p< 0.01, * = p < 0.05. **(H)** Fold change in WT vs *chrna3*^{C246X} of *chrna5* (n = 21/20) and *chrnb4* (n = 22/22) by qRT-PCR. Stars indicate significant difference between genotypes, ** = p< 0.01, * = p < 0.05. **I-K.** Subsets of volcano plot **C**, highlighting genes associated with nicotine **(I)** or alcohol **(J)** dependence [53], and anxiety phenotypes **(K)** [54,55]. The full gene lists and enrichment analysis of these sets can be found in Figure S10 and Tables S14 and S15.

Discussion

In this study we reported the characteristics of the biphasic response of zebrafish to alcohol, aligning it with similar observations in other vertebrates [56,57]. The presence of a hormetic response to alcohol in fish that has been previously described in birds and mammals, makes hormesis a fundamental characteristic that has been in most organisms where this has been examined [58]. Such biphasic responses to external agents are common, applicable equally to the perceived pleasantness of an odour as it is to concentration-dependent effectiveness of a pharmacological agent [58,59]. The closed-loop design of SAZA allowed examination of uninhibited choice of subject fish, similar to the two-bottle choice assay used in rodents. Using an improved design of SAZA that revealed this biphasic response to alcohol in zebrafish, also isolated the role of *chrna3* within this response.

Shoaling behaviour in zebrafish, which is established by 14 dpf [60], is ideal to study the biphasic effects [51,61,62] of alcohol acting both as a stimulant and a sedative depending on the concentration [27,52]. Immersion is a unique alcohol administration route available for fish, causing a progressive increase in blood alcohol concentration (BAC) with time [63]. BAC is a key measure affecting the physiological responses of animals. The BAC of larval zebrafish (7-10 dpf) reaches 0.04% with 1 minute of immersion in 1.5% alcohol, doubling to 0.08% in 10 minutes [63]. In both humans and zebrafish, BAC > 0.05%, the equivalent of ~2-3 Australian "standard drinks", results in significant behavioural impairment. In humans, this is in the form of slower reaction times [64] and in zebrafish, it manifests as a loss of swimming coordination or impaired swim speeds [24,65]. Immersion in lower concentrations (0.25% to 0.5%) however, is stimulatory in adult zebrafish, activating dopaminergic reward pathways as well as increasing locomotion while reducing anxiety-like behaviours and aggression [49,66]. In our study, both 0.5% and 1% alcohol reduced shoal cohesion but they differed in effect on shoal kinesis (Figure 5). This suggests that a reduction in shoal cohesion alone in this assay reflects a reduced anxiety-like condition, while an accompanying reduction in kinesis is indicative of the disruptive, sedative effects of alcohol. As the juvenile fish of this age are smaller in size (~8-12mm length, compared to ~30-40mm length in adults), the BAC is expected to reach the same level as adults faster [63]. Given the matching alcohol

concentrations and exposure durations within the shoal cohesion and SAZA assays, BAC exceeding 0.05% likely results in reduced shoal kinesis and avoidance behaviours respectively.

In humans, individual variability is proposed to have a strong influence on the shift between attraction and aversion. This is similar to the diminished effect of alcohol on 'bold' zebrafish compared to their 'shy' counterparts [49]. However, despite this natural response variability, the population response in SAZA switched from preference to avoidance as the concentration of alcohol increased from < 0.5% to > 0.7% (Figure 2). This switch aligned with the concentration and effect of alcohol in the shoaling cohesion assay and also parallels adult zebrafish consuming greater quantities of 10% alcohol-infused gelatin compared to 20% alcohol-infused gelatin [31]. This tolerance window potentially suggests the existence of a signalling response threshold governing the switch from attraction to aversion. Grasing (2016) [67] proposed a twin threshold model where enhancing the cholinergic signal in ventral tegmental area (VTA) and nucleus accumbens (NAc) can reduce, or enhance behaviours reinforced by drugs of abuse. In this model, passing the lower acetylcholine signalling threshold increases the probability of positive reward association and repetition of the behaviour, while crossing a second, higher threshold diminishes them [67]. This model may be more broadly applicable to include medial habenula (MHb) cholinergic circuit function that predominantly express α3β4 nAChR receptors. These receptors have a lower binding affinity to many agonists including nicotine and could thus also have a higher threshold of activation [68].

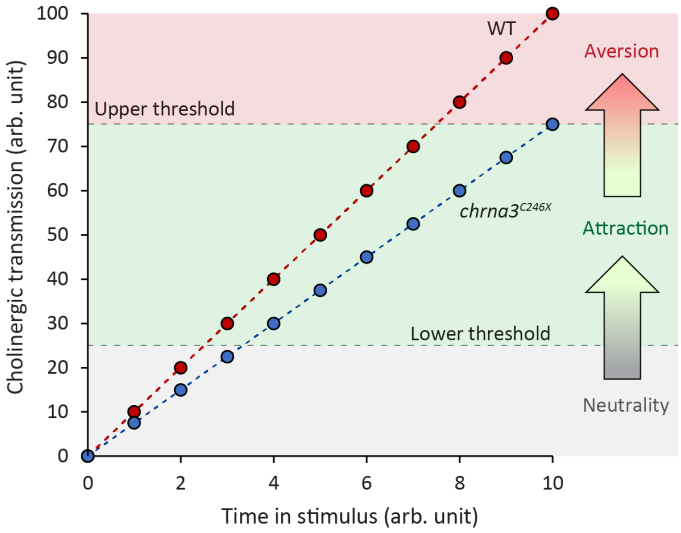

Figure 7. Cartoon of the twin threshold model. Hypothetically reduced cholinergic signalling in *chrna3*^{C246X} mutants results in a shallower slope, causing delayed response switching, with the difference between genotypes being more easily observable at the upper threshold than the lower.

The medial habenula (MHb in mammals or the DHb, dorsal habenula in zebrafish) - interpeduncular nucleus (IPN) circuit is associated with aversive and withdrawal responses to drugs and nicotine [37,69–71]. This has been well studied in rodents in response to nicotine and alcohol, where disrupting MHb - IPN transmission typically results in increased drug intake [37,40,72,73]. The MHb-IPN circuit is also a site of high expression of the three nAChR subunits α3, α5, and β4 encoded by the *CHRNA5-A3-B4* gene cluster, thus suggesting a central role for these subunits in mediating the aversion to psychoactive substances [40,73,74]. In rodents, overexpression of *Chrnb4* or *Chrna5* of this gene cluster results in reduction in the quantities of ethanol self-administered in acute conditions, implying cholinergic signs here acts as a 'brake' on drug consumption [74]. Knockouts of *Chrna3* are non-viable [39]. Only one study in rodents used conditional knockout of *chrna3* [40] to examine effect in nicotine response. Zebrafish, however, do not require *chrna3* in the periphery, and mutants survive to

adulthood in the homozygous condition. As such the zebrafish made for an excellent candidate to assess the role of this gene in alcohol preference.

Broadly, the *chrna3* mutation here appeared to blunt the aversive switch in the biphasic response but maintained the attractive response (Figure 2, 4). Whilst wild-type fish exhibited aversive behaviour to > 0.7% alcohol, the mutants did not. This is corroborated with rodent studies, where knockdown of *Chrna3*, or blocking of α3β4 receptors with the non-specific nAChR antagonist 18-methoxycoronaridine (18-MC) in the MHb - IPN resulted in reduced transmission and increased self-administration of nicotine or alcohol, respectively [72,73]. The increased tolerance exhibited by mutants, however, had limits and alcohol >~1.6% triggered an aversive response (Figure 3, 4). The delayed onset of aversion exhibited by *chrna3*^{C246X} fish could then be attributed to reduced cholinergic transmission, increasing the dose required to cross the upper threshold. Once the upper threshold is reached, however, the aversive response is mounted as per normal (Figure 7). The window of increased tolerance also correlated with the disparate effects of 0.5% alcohol on shoal cohesion between the two genotypes (Figure 5). The c*hrna3* mutants retained significantly greater shoal cohesion following extended immersion, indicating a reduced anxiolytic effect of alcohol (Figure 5H), even though they showed parity in the first five minutes of 0.5% alcohol immersion (Figure S9). This initial parity was similar to the early attractive response of WT and mutants to x̄0.5% SAZA (Figure 3, 4). Apart from placing *chrna3* as a key factor in acute tolerance, these results also showed that responses in SAZA closely tracked the effect alcohol has on behaviour.

Alcohol-induced kinesis was also altered between the genotypes. The *chrna3*^{C246X} mutant fish exhibited a stronger alcohol-induced locomotor response to alcohol in both the SAZA and shoaling cohesion assays (Figure 5, S5). We observed expression of *chrna3* in the caudal, rostral, and supra-rostral regions of the facial motor nucleus (Fmn), also termed the octavolateral efferent nucleus (OEN), by HCR (Figure 3). Expression of *chrna3* in this region was significantly reduced in mutants (Figure S4). This region of the hindbrain connects to the lateral line, and the cholinergic signalling in this system is hypothesised to act as a 'brake' on locomotor auto-sensory stimulation, limiting the response to constitutive excitation generated during swimming [75–77]. While typically this function is assigned to α9 receptors, if α3 does play a role centrally as suggested recently [78], then it may account for the heightened alcohol-induced locomotor response observed in *chrna3*^{C246X} mutants. The influence of *chrna3* on locomotor control however, needs further investigation as the existing evidence in rodents is inconsistent [44].

Although it is not possible to implicate a specific brain region, such as the dHb in our study as *chrna3*^{C246X} fish harboured a whole-body mutation, they can be useful to mimic the functional consequences of harbouring *CHRNA3* SNP variants in humans. RNA sequencing of the whole brain in our study highlighted that broad, large scale transcriptional changes occurred in the mutants. The upregulation of genes associated with nicotine dependence [53] was small but consistent (Figure 6). This is indicative of a bidirectional relationship as several GWAS studies link polymorphisms in *CHRNA3* with nicotine dependence [79,80]. The downregulation of *chrna5* and *chrnb4* (Figure 6K) is notable as these genes are co-expressed with *chrna3* in other vertebrates and have individually been associated with substance dependence [37,38]. Co-regulation of these genes may also be a contributing factor in the alcohol tolerance phenotype observed in the *chrna3*^{C246X} mutants. In addition to nAChRs, alcohol impacts both glutamate and GABA receptor functions changing the excitatory and inhibitory tone, respectively, eventually

resulting in reduced signal transmission and sedation [81–83]. It was therefore interesting to note that apart from nicotinic receptor genes, mutant brains also had changes in expression of glutamate and GABA receptor genes (Figure 6D, 6E), many of which also feature in nicotine dependence and anxiety phenotype (Figure 6J, 6K). Several expected GO terms such as synaptic signalling, ion channel function, and cation homeostasis were significantly enriched (Figure 6). In addition, unexpectedly, neural development terms such as neuron projection, dendrite development, and axon guidance were also enriched despite the sequenced brains being taken from adult fish (Figure 6B). Finally, genes associated with feeding behaviour as an enriched set was interesting to observe (Figure 6B). Cholinergic signalling has been previously associated with appetite regulation, and SNPs in the CHRNA5-CHRNA3-CHRNB4 cluster have been tentatively linked in the interaction between smoking and obesity by GWAS studies [84–86]**.** These may require further closer examination which may point towards the same genetic factors influencing substance dependence and other comorbid disorders. Altogether, our results reflect that brain-wide compensatory changes occur due to loss of *chrna3* expression affecting several neural processes which, in combination, result in the alcohol tolerant phenotype observed.

Given the current paucity of animal model data on the impact of CHRNA3 in alcohol dependence, and only correlational associations provided by GWAS [35], the evidence of isolated gene function from a whole body mutation in zebrafish presented here thus represents a valuable step forward.

Conclusions

To effectively address Alcohol Use Disorder (AUD), a comprehensive understanding of alcohol's rewarding and aversive properties is imperative. While zebrafish have emerged as a valuable model organism for drug research due to neural conservation and experimental tractability, contingent assays for studying substance use disorders in this species remain limited. Here, we build on the SAZA to characterise the dynamic decision-making in juvenile zebrafish. Our findings reveal a previously undocumented rapid inversion of preference to alcohol. We establish a correlation between this alcohol response in the SAZA and the dual effects of alcohol. Notably, we identify a critical role for the *chrna3* gene in modulating alcohol tolerance, demonstrating a distinct tolerance window. These results provide a robust foundation for elucidating the genetic and neurobiological mechanisms underlying AUD and inform the development of targeted therapeutic interventions.

Materials & Methods

Fish husbandry

Zebrafish (*D. rerio*, ABWT) were housed, bred, and reared as described by Nathan *et al.*, 2022[30] at the ZebraFish Facility (Institute of Molecular and Cell Biology, A*STAR) in groups of 20–30 in 3-L tanks under standard facility conditions. All experimental protocols involving zebrafish were approved by the Institutional Animal Care and Use Committee (IACUC) of the Biological Resource Center at A*STAR. Approved experimental protocols (IACUC #201529, # 231808) were followed.

Generation of c*hrna3* mutant zebrafish

The full details of zebrafish gene editing by CRISPR/Cas9 have been described by Hwang *et al.*[87]. CRISPR targets were determined using the web tool ‘chop-chop’, for the exon 5 region to disrupt key functional

domains. Primers for generating sgRNA are detailed in Table 1. Zebrafish embryos (nacre background) were injected at the 1-cell stage with 1 nL of a mixture containing 1 µL sgRNA (≈ 4-5 µg) and 1 µL Cas9 mRNA (≈1 µg). Fish were genotyped by fin-clipping and sequencing of genomic DNA at 10 weeks post-injection to identify founder fish (F0). The identified founder fish were outcrossed to AB WT fish to obtain F1 embryos. F1 embryos from each outcrossed family were collected and some of the embryos were genotyped. Once germline transmission was confirmed, the remaining embryos were grown to adulthood. Homozygous *chrna3*$^{C246X/C246X}$ mutants from the F3 generation onwards were used for all subsequent experiments, henceforth referred to as *chrna3*^{C246X}.

Table 1. Primers for single-guide RNA template. CRISPR targets are underlined

Gene	Label	Primer 5' ➔ 3'
chrna3	CRISPRT1 (F)	AATTAATACGACTCACTATAGGCTGTCTTCTCATCTCCTTCCGTTTTAGAGCTA GAAATAGC
chrna3	CRISPRT2 (F)	AATTAATACGACTCACTATAGGCCGGTTTCCAGCAAACAGACGTTTTAGAGCT AGAAATAGC
chrna3	CRISPR Universal (R)	TTTTGCACCGACTCGGTGCCACTTTTTCAAGTTGATAACGGACTAGCCTTATT TTAACTTGCT ATTTCTAGCTCTAAAAC

Self-administration for zebrafish assay (SAZA) apparatus setup

The SAZA assay apparatus was set up as described in [30], outlined briefly as follows. The assay tank was constructed of opaque, 3mm thick acrylic to be 35 x 75 x 30mm (width × length × height). One end of the zone contained a dividing sheet of the same material, 30mm in length, to split the zone into two halves while still permitting access (Figure 1A). The zone was placed on an LED lightbox for illumination, providing 5000 lux at maximum intensity (LightPad LX Series, Artograph, USA). Video footage was captured at 30 frames per second using an acA2040-90µM USB3.0 Basler camera. Solutions were dispensed from vertically mounted 10ml syringes through silicon tubing (outer diameter: 1/16", inner diameter 1/32") into the corner of their designated zone, mediated via solenoid pinch valves (Automate Scientific, USA, SKU: 02-pp-04i) (Figure 1A). System water was consistently supplied to the tank through additional silicon tubing at the opposite end of the tank to the divided zones and was removed at a matching rate (~2ml per minute) by gravitational siphoning from the end of the dividing sheet near the centre of the tank (Figure 1A). This created a consistent flow and stopped dispensed solutions from escaping their designated zones while permitting access to the fish being assayed (Figure S1). CRITTA (http://www.critta.org), a custom LABVIEW software, was used to track fish movements as described by Krishnan *et al.* (2014) [88]. The tracking system was configured so that only the entry of the fish to a designated region of interest would trigger the pinch valve to release and dispense the corresponding solution.

Alcohol concentration measurement

Alcohol concentrations in the SAZA stimulus zone were measured using a DensitoPro (Mettler-Toledo), returning the measured solution to the zone with minimal disturbance. As attempting to measure the concentration of alcohol during a live fish assay would disturb the fish and prevent a natural response, an artificial dispensing scheme of ten continuous seconds per minute followed immediately by measurement was used as a substitute (Figure 1C). This was based on the average time fish spent in the stimulus zone under assorted alcohol dispensing solutions over 18 minutes of exposure (Table S1). After 12 minutes, the dispensing cycle was halted, but measurements continued to estimate the effect the outflow rate had on concentration in the zone if no stimulus was dispensed for a long period.

The assay was repeated three times per concentration of alcohol (20, 70%).

SAZA

SAZA was performed as described in [30], outlined briefly as follows. First, 40 ml of system water was added to the tank, the in and outflow tubes were inserted into their respective conditions, and the flow of system water started. One zebrafish of 30-35 dpf was taken directly from its husbandry tank and added gently to each SAZA tank, then given ~5 minutes to adjust and recover post-transfer until consistent swimming behaviour had resumed and the fish had explored all zones of the SAZA tank. The recording and tracking scheme was then started for 24 minutes, consisting of three consecutive periods; three minutes of pre-exposure, 18 minutes of self-administration stimulus delivery, and three minutes post-exposure. Only during the 18-minute stimulus delivery period would entry to a designated zone trigger dispensing of the corresponding solution (Figure 1A). The valve opening time was set to a minimum of five seconds per entry. The stimuli delivered were 0/20/70% absolute alcohol diluted in the facility system water. Following each assay, the zone was emptied of all liquid, washed, and refilled before adding the next fish. The volume of each solution dispensed was also recorded. To reduce bias, the zone designated to deliver the stimulus solution was randomly assigned to be either the left or right and changed periodically throughout the experiment such that ~50% of the fish were tested in each configuration. Around 30 fish naive to SAZA were assayed per concentration of alcohol. Following each assay, the fish were euthanized.

SAZA Data analysis

SAZA data outputs from CRITTA were processed by custom Python scripts. These provided data on time spent in each zone and mean velocity in each zone used in these analyses. The data were separated into three major time groups; pre-exposure, total stimulus delivery period, and post-exposure. The stimulus delivery period was then further subdivided into either start and end (0-9m/9-18m), or three minute segments (0-3m/3-6m/6-9m, etc…) for further analyses.

The preference index for a period (PI_X) was calculated by the following formula; PI_X = (TinS - TinC) / (TinS + TinC), where TinS = time in stimulus zone (s) and TinC = time in control zone (s). This gives the value for PI maximum bounds of + or - 1 indicating more time spent relatively in the stimulus or control, respectively. For example, a PI of +1 would indicate 100% of relative time spent in the stimulus zone during one time period. Delta PI between two time periods (ΔPI_{X-Y}) was calculated as $\Delta PI_{XY} = PI_Y - PI_X$, where PI_X = the earlier period, and PI_Y = the later period. This gives the value for ΔPI maximum bounds of

+ or - 2, with the values indicating the direction and magnitude of the change in preference from the first time point to the second. For example, a ΔPI of +2 would indicate a change from 100% relative time spent in the control zone in the first period, to 100% relative time spent in the stimulus zone in the second. Sparklines were also generated to display the number of entries to each zone, and the duration of each (Figure 1A).

Shoaling cohesion assay

The shoaling cohesion assay apparatus was set up as described for SAZA, with the following alterations. The tank had no dividing sheet, or inflow, outflow, and stimulus dispensing tubing (Figure 4A). Additionally, the tracking of fish movements was not performed. To perform the assay, the tank was half-filled with 20 ml of system water, then four zebrafish of 30-35 dpf were taken directly from their husbandry tank and added gently to each shoaling cohesion tank. The fish were then given ~5 minutes to adjust and recover post transfer until consistent swimming behaviour had resumed. Following this acclimation period, 20 ml of 2x concentration alcohol solution was added to the tank to achieve the 1x desired concentration for the assay. Recording began immediately and continued for 30 minutes. Six repeats were performed per alcohol concentration. Following each assay, the fish were euthanized.

Shoaling cohesion data analysis

Video analysis was performed in imageJ. First, videos were either trimmed to the first 15 minutes, then frames were extracted at 2fps to create an image stack (900 per assay), or one frame per 10 seconds of footage was extracted from the full 30-minute duration (180 per assay). The image stacks for each assay were cleaned using median background subtraction, then converted to 8-bit and auto-thresholded (Figure 4A). From the thresholded images, particles were detected (size = 100-infinity), and the centerpoint of each was determined. Using the centerpoints, Delaunay triangulation was performed on each image to draw triangles covering the space between all four fish. The area of these triangles was then combined to obtain the total area between the fish, as a measure of shoaling cohesion. These area values were grouped into either total time for the full 30 minute duration (n = 1080 per treatment), or one minute intervals for the first 15 minute data (n = 720 per time point per treatment). Values over 2000 mm^2 were identified as products of processing errors and removed (~2.5%).

As a measure of shoal kinesis, the distance travelled by the shoal centerpoint was calculated using the X and Y coordinates for the centerpoint of the triangulation area, as calculated by imageJ, with the equation; distance = $\sqrt{((X_2 - X_1)^2 + (Y_2 - Y_1)^2)}$. X_2 and Y_2 were the subsequent coordinates, 0.5s after X_1 and Y_1, respectively. This provided the distance the shoal centerpoint had travelled between each selected frame. Values over 10 mm per 0.5s were discarded as products of processing errors, as the highest velocities recorded by individual fish were ~20mm/second (Figure 3B). This amounted to < 5% of the data. These values were grouped into one minute intervals for the first 15 minute data (n = 720 per time point per treatment).

Quantitative PCR (qPCR)

Three-month old adult zebrafish were euthanized and the brains were dissected in PBS pH7.0. Brain tissue was homogenised using a micro tube homogenizer (Thomas Scientific) in a lysis buffer made up of Trizol (ThermoFisher #15596026). RNA was extracted using PureLink® Micro Kit (ThermoFisher #K310250) according to the manufacturer's protocol. The concentration and purity of the extracted RNA were determined by NanoDrop™2000 Spectrophotometer (ThermoFisher). Each brain sample yielded around 100 ng/µL RNA with a ratio of absorbance reading 1.9-2.0 at 260/280 nm. The purified RNA was reverse transcribed by SuperScript II First strand Synthesis System (Invitrogen #18091050) using 100 ng/µL of purified RNA to obtain approximately 1000 ng/µL of first strand cDNA. To check for genomic DNA contamination, a negative RT (no reverse transcriptase) was set up for each sample.

The cDNA was diluted with nuclease-free water to 100 ng/µL. The qRT-PCR amplification mixtures (20 µL) contained 100 ng of cDNA, 10 µL 2x GoTaq®qPCR Master Mix (Promega #TM318), and 300 nM forward and reverse primer. The primers used were designed using Primer3 (v.0.4.0) is detailed in Table 2.

Table 2. Primers used for qPCR of *chrna3*, and housekeeping genes.

Gene Accession #	Gene symbol	Primer 5' ➔ 3'
β-actin1 NM_131031.2	*actb1*	(F) AGATGACACAGATCATGTTCGAGA (R) CCAGTAGTACGACCAGAAGCG
Elongation factor I-alpha FJ915061.1	*ef1a*	(F) CTGGAGGCCAGCTCAAACAT (R) ATCAAGAAGAGTAGTACCGCTAGCATT
chrna3 ENSDARG00000100991.2	*chrna3*	(F) CCTCCTGTGTCCGACTGAAC (R) CTTCCAGTCATCCTGGACCTC

Reactions were performed using a 7500 Real-Time PCR system (Applied Biosystems) in 96-well plate format. The cycling conditions were as follows: 95°C for 10m to activate, then 40 cycles of 95°C for 15s, 60°C for 30s. After completion, a melt curve was run at 65-95°C for 5 seconds per step. All PCR efficiencies were above 95%. Primer specificity was validated by a single peak on the post-PCR melt curve and single-band after electrophoresis.

The relative gene expression levels were analysed using the adjusted delta-delta CT method described by Hellemans and Mortier et al. (2007). All data were analysed by one-way ANOVA, with genotype as the independent variable and target gene expression, relative to reference genes, as the dependent variable. For mRNA relative expression data, adjusted *p* values were estimated using Dunnett post-hoc tests. Effect sizes for all differences in expression were also calculated using Cliff's Delta statistics as described below.

Statistical analyses

Data was analysed and presented following the principles outlined by Ho *et al.* (2019), to which a P value as a measure of significance is improved upon by the supplementary reporting of effect sizes, means, and 95% confidence intervals [89]. As the typical assumptions of parametric testing could not be consistently met, groups were compared by non-parametric two-sided permutation T-tests (5000 reshuffles) with a significance level of 0.05, and unpaired Cliff's delta in R using the 'dabestr' package. All statistical analysis outputs can be found in supplementary tables. This data was presented in the form of Gardener-Altman and Cummings estimation plots. Results are reported as Cliff's delta = X, 95% CI [lower, upper], p = Y. Cliff's delta effect sizes greater than ± 0.4 and a p-value of < 0.01 was considered meaningful and practically relevant in this study. Smaller Cliff's delta effect sizes of ± 0.2 to 0.4 with accompanying p-value of < 0.05 were also considered potentially meaningful, but provisional pending experimental reproduction [90].

Hybridisation chain reaction, RNA-fluorescent in-situ hybridisation (HCR™ RNA-FISH)

HCR™ RNA-FISH 3.0 (HCR) (Choi et al. 2018) probes against chrna3, chata, and nrp1a were prepared using an in-house Excel-based program and synthesized by IDT (please see Table S16 for details). The in-situ hybridization experiments were carried out in a controlled incubation chamber (40°C temperature and > 90% humidity). Briefly, 10 dpf zebrafish embryos were euthanized and fixed in 4% formaldehyde diluted in 1X PBST at room temperature for 60 minutes with shaking. The larvae were washed with 1X PBST for 3 minutes x 3 times. Embryos were permeabilized using a detergent solution (1% SDS, 0.5% Tween 20, 150mM NaCl, 1mM EDTA, 0.05M Tris-HCL, pH 7.5) at 37°C for 30 minutes. They were washed for 3 minutes x 3 times each with 1X PBST and then 5X SSCT. Larvae were transferred to 30% probe hybridization buffer (30% formamide, 9mM citric acid, 0.1% Tween 20, 50µg/mL heparin, 1x Denhardt's solution, 5X SSC) and incubated at 37°C for 30 minutes. Simultaneously, probes were prepared in a solution containing 30ul (10uM) of probe set against each gene in 1000 µl of 30% probe hybridization buffer. The larvae were either transferred to the robotic chamber or a 1.5ml centrifuge tube for automated or manual experiments. Larvae were incubated with the probes at 37°C for 8-12 hrs. For both methods, on day 2, larvae were washed 5 times with 30% probe wash buffer (30% formamide, 9mM citric acid, 0.1% Tween 20, 50µg/mL heparin, 5x SSC) at 37°C and then 5X SSCT twice. For the secondary reaction, HCR hairpins (Molecular Instruments) were diluted and prepared in an amplification buffer (5X SSC, 0.1% Tween 20, 2.5% dextran sulphate) and incubated overnight (for the manual methodology) or 3 hours (for the automated) in the dark. The larvae were then washed with 5X SSCT, 4 X 10 mins each in the dark. They were mounted with the cover slip on the dorsal side in 70% glycerol-based mounting media and imaged on an Olympus FV3000 confocal microscope with the settings consistent between fish. Images were post-processed first on Olympus viewer FLUOVIEW FV31S-SW software with linear intensity adjustments of 150 - 4095 for all genes. Images presented for *nrp1a*, *chata* and *chrna3* had no further processing beyond cropping to the ROI and addition of scale bars. The *elavl3* and *chrna3* false colour images were processed in Imagej. The *elavl3* images had additional linear brightness/contrast adjustment (15 - 110). False colour images were converted to 8bit and had the 'fire' LUT applied, followed by linear brightness/contrast adjustment of 0 - 175, background subtraction with 25px rolling ball, and 1px gaussian blur.

RNAseq

RNA was extracted from *chrna3*^{C246X} and WT brains in triplicate as described previously. The quality of each sample was verified by gel electrophoresis and bio-analyser. Samples that passed QC were sent for sequencing by Novogene AIT. An mRNA cDNA library made up of Paired-end sequencing reads of 150 bp in length was generated on the Illumina HiSeq instrument. Raw reads were first processed by Novogene-AIT to remove adapter, poly-N sequences, and reads with low quality from raw data. All downstream analyses were based on the clean data with a Phred score of 39 indicating a 99.9% base call accuracy. Further analysis was performed in Partek™ Flow™ Explore Spatial Multiomics Data using Partek™ Flow™ software, v11.0. Reads were aligned to GRCz11 genome assembly by STAR aligner, default parameters, and subsequently filtered to a minimum mapping quality score of > 30. Gene counts were normalised by median ratio, followed by differential expression analysis in DeSeq2. Significance thresholds were set as follows: up/down-regulated genes = $p < 0.05$ & fold change > ±2. Provisional up/down-regulated genes = $p < 0.05$ & fold change < ±2. Non-significant genes = $p > 0.05$. Custom gene lists and sets for analysis can be found in Table S14. Gene set enrichment analysis (GSEA) was performed using the GRCz11-GO database, 100 permutations. Significance thresholds were set at $p < 0.05$ and FDR < 0.2.

Supplementary Materials:

Video S1: Video clip shows a segment of SAZA with $\bar{x}$1.5% shown in Figure 1B. Video S2: Video clip showing shoaling assay with 1% alcohol. Supplementary Material Figures S1-S10, Tables S1-S16

Author Contributions:

Conceptualization, A.S.M, and J.R; methodology, A.S.M., T.D.B., C.K., and J.R.; formal analysis, J.R., T.D.B and A.S.M.; investigation, J.R., C.K., and A.S.M; resources, A.S.M; writing—original draft preparation, J.R, and A.S.M.; writing—review and editing, All.; visualisation, J.R.; supervision, A.S.M.; project administration, A.S.M., A.M.; funding acquisition, A.S.M.

Funding:

This research was funded by the Ministry of Education (MOE), Singapore (through grant number T2EP30220-0020), and Yale-NUS College (through grant numbers IG16-LR003, IG18-SG103, IG19-BG106, and SUG) to ASM.

Data Availability Statement:

The datasets used to generate the figures are included within the article and its additional file(s). Additional data are available from the corresponding author upon request.

Acknowledgments:

We would like to thank the zebrafish fish facility staff at the IMCB, A*STAR for their assistance with fish husbandry. We also thank Li Xinrui for generating customized Python analysis scripts.

Conflicts of Interest:

The authors declare no conflict of interest. The sponsors had no role in the design, execution, interpretation, or writing of the study.

References:

1. Witkiewitz, K., Litten, R. Z. & Leggio, L. Advances in the science and treatment of alcohol use disorder. *Sci Adv* **5**, eaax4043 (2019).
2. Moeller, G. & Terplan, M. *Substance Use Disorders*. (Oxford University Press, USA, 2020).
3. Rehm, J. & Shield, K. D. Global Burden of Disease and the Impact of Mental and Addictive Disorders. *Curr. Psychiatry Rep.* **21**, 10 (2019).
4. Aslam, A. & Kwo, P. Y. Epidemiology and Disease Burden of Alcohol Associated Liver Disease. *J. Clin. Exp. Hepatol.* **13**, 88–102 (2023).
5. Rehm, J. & Shield, K. D. Global Burden of Alcohol Use Disorders and Alcohol Liver Disease. *Biomedicines* **7**, 99 (2019).
6. Hirode, G., Saab, S. & Wong, R. J. Trends in the Burden of Chronic Liver Disease Among Hospitalized US Adults. *JAMA Netw Open* **3**, e201997 (2020).
7. Carvalho, A. F., Heilig, M., Perez, A., Probst, C. & Rehm, J. Alcohol use disorders. *Lancet* **394**, 781–792 (2019).
8. Yang, W., Singla, R., Maheshwari, O., Fontaine, C. J. & Gil-Mohapel, J. Alcohol Use Disorder: Neurobiology and Therapeutics. *Biomedicines* **10**, 1192 (2022).
9. Egervari, G., Siciliano, C. A., Whiteley, E. L. & Ron, D. Alcohol and the brain: from genes to circuits. *Trends Neurosci.* **44**, 1004–1015 (2021).
10. Hitzemann, R. *et al.* Sex Differences in the Brain Transcriptome Related to Alcohol Effects and Alcohol Use Disorder. *Biol. Psychiatry* **91**, 43–52 (2022).
11. Koob, G. F. & Vendruscolo, L. Theoretical Frameworks and Mechanistic Aspects of Alcohol Addiction: Alcohol Addiction as a Reward Deficit/Stress Surfeit Disorder. *Curr. Top. Behav. Neurosci.* (2023) doi:10.1007/7854_2023_424.
12. Smith, M. A. Nonhuman animal models of substance use disorders: Translational value and utility to basic science. *Drug Alcohol Depend.* **206**, 107733 (2020).
13. de Magalhães, J. P. The big, the bad and the ugly: Extreme animals as inspiration for biomedical research. *EMBO Rep.* **16**, 771–776 (2015).
14. Cox, T. C. Utility and limitations of animal models for the functional validation of human sequence variants. *Mol Genet Genomic Med* **3**, 375–382 (2015).
15. Kalueff, A. V., Stewart, A. M. & Gerlai, R. Zebrafish as an emerging model for studying complex brain disorders. *Trends Pharmacol. Sci.* **35**, 63–75 (2014).
16. Cully, M. Zebrafish earn their drug discovery stripes. *Nat. Rev. Drug Discov.* **18**, 811–813 (2019).
17. Bonan, C. D. & Siebel, A. *Zebrafish as a Model for Pharmacological and Toxicological Research*. (Frontiers Media SA, 2022).
18. Drinks like a fish: zebra fish (Danio rerio) as a behavior genetic model to study alcohol effects. *Pharmacol. Biochem. Behav.* **67**, 773–782 (2000).

19. Gerlai, R. Evolutionary conservation, translational relevance and cognitive function: The future of zebrafish in behavioral neuroscience. *Neurosci. Biobehav. Rev.* **116**, 426–435 (2020).
20. Kily, L. J. M. *et al.* Gene expression changes in a zebrafish model of drug dependency suggest conservation of neuro-adaptation pathways. *J. Exp. Biol.* **211**, 1623–1634 (2008).
21. Vaz, R., Hofmeister, W. & Lindstrand, A. Zebrafish Models of Neurodevelopmental Disorders: Limitations and Benefits of Current Tools and Techniques. *Int. J. Mol. Sci.* **20**, 1296 (2019).
22. Cassar, S. *et al.* Use of Zebrafish in Drug Discovery Toxicology. *Chem. Res. Toxicol.* **33**, 95–118 (2020).
23. Patton, E. E., Zon, L. I. & Langenau, D. M. Zebrafish disease models in drug discovery: from preclinical modelling to clinical trials. *Nat. Rev. Drug Discov.* **20**, 611–628 (2021).
24. Tsang, B., Ansari, R. & Gerlai, R. Dose dependent behavioral effects of acute alcohol administration in zebrafish fry. *Pharmacol. Biochem. Behav.* **179**, 124–133 (2019).
25. McKendrick, G. & Graziane, N. M. Drug-Induced Conditioned Place Preference and Its Practical Use in Substance Use Disorder Research. *Front. Behav. Neurosci.* **14**, 582147 (2020).
26. Echevarria, D. J., Toms, C. N. & Jouandot, D. J. Alcohol-induced behavior change in zebrafish models. *Rev. Neurosci.* **22**, 85–93 (2011).
27. Kurta, A. & Palestis, B. G. Effects of Ethanol on the Shoaling Behavior of Zebrafish (Danio Rerio). *Dose Response* (2010) doi:10.2203/dose-response.10-008.Palestis.
28. Schneider, H. *et al.* Identification of nicotine-seeking and avoiding larval zebrafish using a new three-choice behavioral assay. *Front. Mol. Neurosci.* **16**, 1112927 (2023).
29. Bossé, G. D. & Peterson, R. T. Development of an opioid self-administration assay to study drug seeking in zebrafish. *Behav. Brain Res.* **335**, 158–166 (2017).
30. Nathan, F. M. *et al.* Contingent stimulus delivery assay for zebrafish reveals a role for CCSER1 in alcohol preference. *Addict. Biol.* **27**, e13126 (2022).
31. Sterling, M. E., Karatayev, O., Chang, G.-Q., Algava, D. B. & Leibowitz, S. F. Model of voluntary ethanol intake in zebrafish: effect on behavior and hypothalamic orexigenic peptides. *Behav. Brain Res.* **278**, 29–39 (2015).
32. Thorgeirsson, T. E. *et al.* A variant associated with nicotine dependence, lung cancer and peripheral arterial disease. *Nature* **452**, 638–642 (2008).
33. Amos, C. I., Spitz, M. R. & Cinciripini, P. Chipping away at the genetics of smoking behavior. *Nat. Genet.* **42**, 366–368 (2010).
34. Bierut, L. J. Genetic vulnerability and susceptibility to substance dependence. *Neuron* **69**, 618–627 (2011).
35. Haller, G. *et al.* Rare missense variants in CHRNB3 and CHRNA3 are associated with risk of alcohol and cocaine dependence. *Hum. Mol. Genet.* **23**, 810–819 (2014).
36. Kamens, H. M., Flarend, G. & Horton, W. J. The role of nicotinic receptors in alcohol consumption. *Pharmacol. Res.* **190**, 106705 (2023).
37. Fowler, C. D., Lu, Q., Johnson, P. M., Marks, M. J. & Kenny, P. J. Habenular α5 nicotinic receptor subunit signalling controls nicotine intake. *Nature* **471**, 597–601 (2011).
38. Frahm, S. *et al.* Aversion to nicotine is regulated by the balanced activity of β4 and α5 nicotinic receptor subunits in the medial habenula. *Neuron* **70**, 522–535 (2011).
39. Xu, W. *et al.* Megacystis, mydriasis, and ion channel defect in mice lacking the alpha3 neuronal nicotinic acetylcholine receptor. *Proc. Natl. Acad. Sci. U. S. A.* **96**, 5746–5751 (1999).

40. Elayouby, K. S. *et al.* α3* Nicotinic Acetylcholine Receptors in the Habenula-Interpeduncular Nucleus Circuit Regulate Nicotine Intake. *J. Neurosci.* **41**, 1779–1787 (2021).
41. Bogdan, R., Hatoum, A. S., Johnson, E. C. & Agrawal, A. The Genetically Informed Neurobiology of Addiction (GINA) model. *Nat. Rev. Neurosci.* **24**, 40–57 (2023).
42. Mathur, P., Berberoglu, M. A. & Guo, S. Preference for ethanol in zebrafish following a single exposure. *Behav. Brain Res.* **217**, 128–133 (2011).
43. Wang, J. C. *et al.* Genetic variation in the CHRNA5 gene affects mRNA levels and is associated with risk for alcohol dependence. *Mol. Psychiatry* **14**, 501–510 (2009).
44. Kamens, H. M. *et al.* The alpha 3 subunit gene of the nicotinic acetylcholine receptor is a candidate gene for ethanol stimulation. *Genes Brain Behav.* **8**, 600–609 (2009).
45. Gotti, C., Zoli, M. & Clementi, F. Brain nicotinic acetylcholine receptors: native subtypes and their relevance. *Trends Pharmacol. Sci.* **27**, 482–491 (2006).
46. Wada, E. *et al.* Distribution of alpha 2, alpha 3, alpha 4, and beta 2 neuronal nicotinic receptor subunit mRNAs in the central nervous system: a hybridization histochemical study in the rat. *J. Comp. Neurol.* **284**, 314–335 (1989).
47. Zhou, X. *et al.* I-TASSER-MTD: a deep-learning-based platform for multi-domain protein structure and function prediction. *Nat. Protoc.* **17**, 2326–2353 (2022).
48. Kunst, M. *et al.* A Cellular-Resolution Atlas of the Larval Zebrafish Brain. *Neuron* **103**, 21–38.e5 (2019).
49. Araujo-Silva, H., Leite-Ferreira, M. E. & Luchiari, A. C. Behavioral Screening of Alcohol Effects and Individual Differences in Zebrafish (Danio rerio). *Alcohol Alcohol* **55**, 591–597 (2020).
50. Gebauer, D. L. *et al.* Effects of anxiolytics in zebrafish: similarities and differences between benzodiazepines, buspirone and ethanol. *Pharmacol. Biochem. Behav.* **99**, 480–486 (2011).
51. Oscar-Berman, M. & Marinković, K. Alcohol: Effects on Neurobehavioral Functions and the Brain. *Neuropsychol. Rev.* **17**, 239–257 (2007).
52. Miller, N., Greene, K., Dydinski, A. & Gerlai, R. Effects of nicotine and alcohol on zebrafish (Danio rerio) shoaling. *Behav. Brain Res.* **240**, 192–196 (2013).
53. Hu, R., Dai, Y., Jia, P. & Zhao, Z. ANCO-GeneDB: annotations and comprehensive analysis of candidate genes for alcohol, nicotine, cocaine and opioid dependence. *Database* **2018**, (2018).
54. Koskinen, M.-K. & Hovatta, I. Genetic insights into the neurobiology of anxiety. *Trends Neurosci.* **46**, 318–331 (2023).
55. Howe, A. S. *et al.* Candidate genes in panic disorder: meta-analyses of 23 common variants in major anxiogenic pathways. *Mol. Psychiatry* **21**, 665–679 (2016).
56. Calabrese, E. J. & Baldwin, L. A. Ethanol and hormesis. *Crit. Rev. Toxicol.* **33**, 407–424 (2003).
57. Calabrese, E. J. & Baldwin, L. A. U-shaped dose-responses in biology, toxicology, and public health. *Annu. Rev. Public Health* **22**, 15–33 (2001).
58. Calabrese, E. J. U-shaped dose response in behavioral pharmacology: historical foundations. *Crit. Rev. Toxicol.* **38**, 591–598 (2008).
59. Agathokleous, E. & Calabrese, E. J. Hormesis: The dose response for the 21st century: The future has arrived. *Toxicology* **425**, 152249 (2019).
60. Miller, N. & Gerlai, R. Quantification of shoaling behaviour in zebrafish (Danio rerio). *Behav. Brain Res.* **184**, 157–166 (2007).

61. Rueger, S. Y. & King, A. C. Validation of the brief Biphasic Alcohol Effects Scale (B-BAES). *Alcohol. Clin. Exp. Res.* **37**, 470–476 (2013).
62. Chvilicek, M. M., Titos, I. & Rothenfluh, A. The Neurotransmitters Involved in Alcohol-Induced Behaviors. *Front. Behav. Neurosci.* **14**, 607700 (2020).
63. Lockwood, B., Bjerke, S., Kobayashi, K. & Guo, S. Acute effects of alcohol on larval zebrafish: a genetic system for large-scale screening. *Pharmacol. Biochem. Behav.* **77**, 647–654 (2004).
64. Grant, S. A., Millar, K. & Kenny, G. N. Blood alcohol concentration and psychomotor effects. *Br. J. Anaesth.* **85**, 401–406 (2000).
65. Tran, S. & Gerlai, R. Time-course of behavioural changes induced by ethanol in zebrafish (Danio rerio). *Behav. Brain Res.* **252**, 204–213 (2013).
66. Echevarria, D. J., Hammack, C. M., Jouandot, D. J. & Toms, C. N. Does Acute Alcohol Exposure Modulate Aggressive Behaviors in the Zebrafish (Danio rerio), or is the Bark Worse than the Bite? *Int. J. Comp. Psychol.* **23**, (2010).
67. Grasing, K. A threshold model for opposing actions of acetylcholine on reward behavior: Molecular mechanisms and implications for treatment of substance abuse disorders. *Behav. Brain Res.* **312**, 148–162 (2016).
68. Coe, J. W. *et al.* Varenicline: an alpha4beta2 nicotinic receptor partial agonist for smoking cessation. *J. Med. Chem.* **48**, 3474–3477 (2005).
69. Antolin-Fontes, B., Ables, J. L., Görlich, A. & Ibañez-Tallon, I. The habenulo-interpeduncular pathway in nicotine aversion and withdrawal. *Neuropharmacology* **96**, 213–222 (2015).
70. McLaughlin, I., Dani, J. A. & De Biasi, M. The medial habenula and interpeduncular nucleus circuitry is critical in addiction, anxiety, and mood regulation. *J. Neurochem.* **142 Suppl 2**, 130–143 (2017).
71. Fowler, C. D. & Kenny, P. J. Habenular signaling in nicotine reinforcement. *Neuropsychopharmacology* **37**, 306–307 (2012).
72. Miller, C. N., Ruggery, C. & Kamens, H. M. The α3β4 nicotinic acetylcholine receptor antagonist 18-Methoxycoronaridine decreases binge-like ethanol consumption in adult C57BL/6J mice. *Alcohol* **79**, 1–6 (2019).
73. Glick, S. D., Sell, E. M., McCallum, S. E. & Maisonneuve, I. M. Brain regions mediating α3β4 nicotinic antagonist effects of 18-MC on nicotine self-administration. *Eur. J. Pharmacol.* **669**, 71–75 (2011).
74. Gallego, X. *et al.* Transgenic over expression of nicotinic receptor alpha 5, alpha 3, and beta 4 subunit genes reduces ethanol intake in mice. *Alcohol* **46**, 205–215 (2012).
75. Pichler, P. & Lagnado, L. Motor Behavior Selectively Inhibits Hair Cells Activated by Forward Motion in the Lateral Line of Zebrafish. *Curr. Biol.* **30**, 150–157.e3 (2020).
76. Odstrcil, I. *et al.* Functional and ultrastructural analysis of reafferent mechanosensation in larval zebrafish. *Curr. Biol.* **32**, 176–189.e5 (2022).
77. Manuel, R., Iglesias Gonzalez, A. B., Habicher, J., Koning, H. K. & Boije, H. Characterization of Individual Projections Reveal That Neuromasts of the Zebrafish Lateral Line are Innervated by Multiple Inhibitory Efferent Cells. *Front. Neuroanat.* **15**, 666109 (2021).
78. Rima, M. *et al.* Dynamic regulation of the cholinergic system in the spinal central nervous system. *Sci. Rep.* **10**, 15338 (2020).
79. Maes, H. H. *et al.* A twin association study of nicotine dependence with markers in the CHRNA3 and CHRNA5 genes. *Behav. Genet.* **41**, 680–690 (2011).

80. Chen, X. *et al.* Variants in nicotinic acetylcholine receptors alpha5 and alpha3 increase risks to nicotine dependence. *Am. J. Med. Genet. B Neuropsychiatr. Genet.* **150B**, 926–933 (2009).
81. Jones, A. W. Alcohol, its absorption, distribution, metabolism, and excretion in the body and pharmacokinetic calculations. *WIREs Forensic Science* **1**, e1340 (2019).
82. Davies, M. The role of GABAA receptors in mediating the effects of alcohol in the central nervous system. *J. Psychiatry Neurosci.* **28**, 263–274 (2003).
83. Möykkynen, T. & Korpi, E. R. Acute effects of ethanol on glutamate receptors. *Basic Clin. Pharmacol. Toxicol.* **111**, 4–13 (2012).
84. Herman, A. M. *et al.* A cholinergic basal forebrain feeding circuit modulates appetite suppression. *Nature* **538**, 253–256 (2016).
85. Ortiz-Guzman, J. *et al.* Cholinergic Basal Forebrain Connectivity to the Basolateral Amygdala Modulates Food Intake. *eNeuro* **11**, (2024).
86. Varga, T. V., Hallmans, G., Hu, F. B., Renström, F. & Franks, P. W. Smoking status, snus use, and variation at the CHRNA5-CHRNA3-CHRNB4 locus in relation to obesity: the GLACIER study. *Am. J. Epidemiol.* **178**, 31–37 (2013).
87. Hwang, W. Y. *et al.* Efficient genome editing in zebrafish using a CRISPR-Cas system. *Nat. Biotechnol.* **31**, 227–229 (2013).
88. Krishnan, S. *et al.* The Right Dorsal Habenula Limits Attraction to an Odor in Zebrafish. *Curr. Biol.* **24**, 1167–1175 (2014).
89. Ho, J., Tumkaya, T., Aryal, S., Choi, H. & Claridge-Chang, A. Moving beyond P values: data analysis with estimation graphics. *Nat. Methods* **16**, 565–566 (2019).
90. Goodman, W. M., Spruill, S. E. & Komaroff, E. A proposed hybrid effect size plus *p*-value criterion: Empirical evidence supporting its use. *Am. Stat.* **73**, 168–185 (2019).